Wavelength and photon dose dependence of infrared quenched persistent photoconductivity in $YBa_2Cu_3O_{6+x}$

Daniel M. Bubb* and J. F. Federici
Department of Physics, New Jersey Institute of Technology, Newark, New Jersey 07102

S. C. Tidrow
Sensors and Electron Devices Directorate, Army Research Laboratory, Adelphi, Maryland 20783

W. Wilber
U.S. Army CECOM, Fort Monmouth, New Jersey 07703

J. Kim and A. Piqué
Naval Research Laboratory, Surface Modification Branch, Washington, D.C. 20375

(Received 19 February 1999)

Infrared quenched persistent photoconductivity (PPC) is studied as a function of wavelength and photon dose in order to investigate a defect structure which may be responsible for PPC in $YBa_2Cu_3O_{6+x}$. It is found that the magnitude of IR quenching saturates quickly as function of visible photon dose, long before the PPC effect saturates. The wavelength dependence is essentially linear below 1.3 eV and saturates above. The photon dose dependence of IR quenching indicates behavior which cannot be explained using a purely oxygen ordering model for PPC. [S0163-1829(99)03633-4]

I. INTRODUCTION

Several years ago the phenomena of persistent photoconductivity[1] (PPC) and photoinduced superconductivity[2] (PISC) were reported in oxygen-deficient $YBa_2Cu_3O_{6+x}$ (YBCO). Subsequent studies were performed as a function of oxygen content[3] with the discovery that the magnitude of the effect is peaked near $x \approx 0.4$ in $YBa_2Cu_3O_{6+x}$. Attempts to explain the mechanism have generally fallen into two classes: (1) photoassisted oxygen ordering,[4] and (2) photoinduced charge-transfer mechanism. In the photoinduced charge-transfer mechanism, an excited electron is trapped either in a CuO_x chain fragment[3] or an oxygen vacancy.[5,6] In both cases, the trapping of an electron is thought to result in the transfer of a hole to the CuO_2 planes where it contributes to the conductivity. In the photoassisted oxygen-ordering model, photons enable the motion of basal plane oxygen atoms to move within the lattice and become part of the CuO_x chains. As these chains lengthen, they inject holes into the CuO_2 planes by acting as charge reservoirs.[7] A statistical calculation[5,6] shows that for very low oxygen contents, almost all of the CuO_x chains are well below the critical length needed to inject holes into the CuO_2 planes. Despite experimental evidence indicating that the efficiency of hole doping is independent of oxygen content,[8] the ability of light to affect the bulk resistivity of the sample is clearly a function of oxygen content.[5,6] The importance of oxygen ordering is evidenced from measurements of photostructural changes[5,6,9–11] on oxygen-deficient samples which mimic those that occur due to reversibly increasing the oxygen content. The effects of oxygen ordering were shown to be linked to the orthorhombic/tetragonal structural phase transition which occurs at 700 K.[12] Also, it was observed in oxygen-deficient YBCO that vacancies in the CuO_x chains tended to order. This ordering was characterized by a large correlation length[13] along the *c* axis in samples with oxygen content close to 6.5. This had been previously observed along the *a* and *b* axes[14] for samples with different O content. In samples quenched rapidly from high-temperature annealing effects were observed even at room temperature.[15] Optical measurements[16] supported the observations by Veal *et al.*, and oxygen ordering was recognized to be of great importance in understanding the optical properties in both the normal and superconducting states of YBCO.

To explain the PPC/PISC effect in terms of oxygen ordering[17,18] it has been proposed that absorbed photons create perturbative electron-hole pairs. The effect of these perturbations is such that the local electric fields and charge distributions are modified, creating dipole moments. These moments cause rearrangement of basal plane oxygen atoms with consequent lengthening of chain fragments. As described previously, once the chain fragments become greater than the critical length, they inject holes into the CuO_2 planes and the bulk conductivity is enhanced. Even in using such a model defects may be necessary to trap photogenerated charges which modify local fields, thus inducing oxygen rearrangement. Variations on percolation models have been suggested[17,19,20] with the common feature being the growth of the CuO_x chains. Once the chains reach a certain length, they touch, forming a percolation path. Recent experimental work has provided some evidence for such a model.[20] For that work, the authors attempt to explain the ac conductivity found by optical conductivity measurements in a region of the phase diagram where dc measurements yield insulating behavior. A simple model for the dielectric function is used. The chains are treated as spherical metallic particles embed-

ded in an insulating matrix. The dielectric function for fully deoxygenated $YBCO_x$ ($x=6.0$) is used to represent the insulating matrix. At some critical point in the phase diagram the metallic particles begin to touch each other and form a percolation path. The transition to overall metallic behavior occurs close to the metal-insulator transition and the orthorhombic-tetragonal structural phase transition ($x=6.35$). Despite excellent agreement between optical measurements of films with extremely low oxygen contents ($x=6.1,6.2$) and numerical calculations, the model remains somewhat problematic in that it no longer applies once the transition to overall metallic behavior occurs. A more complete description would require a forbidding calculation for higher oxygen contents[20] ($x>6.3$) and would not allow the model to remain as simple, i.e., metallic particles in an insulating matrix. However, it must be noted that the authors establish a strong correlation between chain length and the optical properties including PPC. To do this, the samples are heated to well above 300 K (300 °C), thereby shortening the chain length while not altering the oxygen content. A lower free-carrier concentration is evident from a reduction of the spectral weight in the midinfrared reflectivity, along with a small blueshift in the peaks. The chain length as a function of temperature is already known from an Arrhenius plot. When PPC is initiated through exposure to visible light the opposite evolution occurs. There is an increase of spectral weight in the midinfrared and a redshift in the peaks. This yields convincing evidence that the chain length is correlated with exposure to visible light. That is, exposure to visible light causes the oxygen atoms to end up in a more ordered and higher conductivity state. Problematic issues with this model and these measurements are that no definitive answers are offered as to the microscopic origin of PPC in YBCO. In this respect there remains a ''black box'' between the initiation of PPC and the lengthening of chain fragments.

Experimental evidence for the photoinduced charge transfer model has been obtained from photoluminescence measurements[21] and photoconductivity measurements[5] on heavily oxygen-deficient $RBa_2Cu_3O_x$ ($R=$Y, Gd) films. In addition to the luminescence measurements, infrared (IR) quenching[22] of persistent photoconductivity suggests that defects are important for PPC in YBCO. When oxygen-deficient YBCO is exposed to visible radiation the resistance is observed to decrease in accordance with the *stretched-exponential* law.[3] This decrease in resistance persists after the light is blocked, indefinitely at low temperature.[1–3] Despite difficulties in determining the saturation value of resistivity,[23] the dynamics, if not the origin of PPC/PISC appear to be well modeled. It was discovered that subsequent to illumination with visible radiation, if the sample was exposed to IR radiation the resistance was observed to increase.[22] Since the observed changes in resistance, though small, were found to be inconsistent with sample heating, it was supposed that this was evidence supporting a defect based model for PPC/PISC. As will be shown, the cutoff wavelength for the onset of IR quenching is about 750 nm (1.60 eV). Illumination with shorter wavelengths causes the resistivity to continue to decrease. Interestingly enough, this coincides with the semiconducting gap[24] in heavily oxygen-deficient $YBa_2Cu_3O_{6+x}$. This effect is observed continuously for photon energies between 1.24 and 1.6 eV. It has been observed for photon energies as small as 0.25 eV.[22] This presents a stumbling block for oxygen ordering models, namely that visible wavelengths order the lattice but subsequent exposure to IR wavelengths disorder it. Additionally, the character of the dc electrical response to IR light depends on whether or not it has been exposed to visible light. The purpose of this paper will be to present wavelength and photon dose dependent studies of IR quenching for oxygen-deficient $YBa_2Cu_3O_{6+x}$. We believe that these results support the notion that trapped carriers play an important role in the PPC/PISC mechanism in $YBa_2Cu_3O_{6+x}$.

II. EXPERIMENTAL DETAILS

The $YBa_2Cu_3O_{6+x}$ samples used in this study were either fabricated at the Army Research Laboratory (ARL), the Naval Research Laboratory (NRL) or Advanced Technology Materials (ATMI). Samples *A* and *C* were grown by pulsed-laser deposition on (100) $LaAlO_3$ substrates at ARL with the details published elsewhere.[21] Both are ~2500 Å thick. Sample *A* had $T_c=88$ K before annealing with transition width $\Delta T_c<1$ K. Sample *A* was annealed in two stages. The first stage was 625 °C in 910 ppm O_2. X-ray-diffraction measurements (XRD) of the *c*-axis length coupled with the 005/006 (Ref. 25) intensity ratio give an oxygen content of 6.6. The sample was then exposed to 4 W (all lines) argon-ion laser light for ~5500 s, or a photon dose of approximately 6×10^{22} while immersed in liquid nitrogen (LN2). As a result of this illumination the sample's resistance changed, $\Delta R/R \sim 1.6\%$. Next, the sample was annealed at 780 °C in 980 ppm O_2 (balance N_2) and allowed to cool to room temperature rapidly. After annealing, the surface resistance was observed to increase from 120 Ω to 2.6 kΩ. XRD showed that the *c* axis grew and the 005/006 intensity ratio changed consistent with a reversible decrease in oxygen content. Now, $\Delta R/R \sim 90\%$ upon illumination. The character of the ρ vs T curve indicated insulating behavior and the final oxygen content was assessed to be 6.26. Sample *C* had similar starting conditions as Sample *A*. It was annealed in argon at 520 °C. Several times it was deoxygenated and annealed in pure O_2. Each time the original surface resistance was recovered. Similar to *A*, XRD measurements give an O content of 6.15.

Sample *B* was fabricated by single liquid source metalorganic chemical vapor deposition in an inverted vertical reactor at ATMI.[26] The substrate was once again (100) $LaAlO_3$. The film was ~1300 Å thick. Sample *B* was annealed in several stages as well. The final stage was at 748 °C. Micro-Raman measurements over several areas of the film gave the O(4) Ag line at 481 cm^{-1} ($+/-2$ cm^{-1}). This places the oxygen content[27] between 6.35 and 6.46. Further, resistivity measurements[14] indicated that the sample had an O content of approximately 6.4. This, coupled with the weakly metallic ρ vs T curve between 77 and 300 K lead us to assign oxygen content 6.4 to this sample.

Samples *D* and *E* were fabricated at the NRL pulsed-laser deposition facility. The substrate, (001) $SrTiO_3$, was fastened to a heater block held at 750 °C during deposition. The O_2 pressure was 320 mT, with laser fluence 1.35 J/cm^2. Sample *D* is 1500 Å thick, which was verified by profilometry. The T_c of the fully oxygenated film is 88.3 K, with $\Delta T_c \sim 1$ K. XRD indicates a value of 6.41 for the oxygen content[25,27]

TABLE I. Summary of characterization data for $YBa_2Cu_3O_{6+x}$ samples.

Sample	c axis length (Å)	Substrate	Oxygen content	Fabrication
A	11.839, [1.35][a]	$LaAlO_3$ (100)	6.26[c]	e
B	N/A (481 cm^{-1})[b]	$LaAlO_3$ (100)	6.4[d]	f
C	11.858, [1.53][a]	$LaAlO_3$ (100)	6.15[c,d]	e
D	11.776	$SrTiO_3$ (001)	6.41[d]	See text
E	11.798	$SrTiO_3$ (001)	6.39[d]	See text

[a][005/006 ratio].
[b]O(4)A_g Raman mode.
[c]Reference 25.
[d]Reference 27.
[e]Reference 21.
[f]Reference 26.

after annealing similar to Sample *C*. For Sample *E*, which is 1000 Å thick, we arrive at 6.39 as the post-annealed oxygen content by the same analysis as sample *D*. These details are summarized in Table I.

Before annealing, gold or silver pads are deposited on the samples. Gold wire is used for leads and silver paste is used to attach the wire to the pads. The samples are mounted on a copper pad with GE varnish as an adhesive. They are then bolted to a cold finger and placed in an optical cryostat. To insure thermal contact Apezion™ grease is used. The samples are cooled and fully immersed in liquid nitrogen (LN_2). For each run, before illumination, the sample's resistivity vs temperature curve is recorded. A current is applied across a bias resistor and a differential voltage across the sample is measured. Any changes from one run to the next would preclude the continued use of the sample. For the measurements of the IR quenching spectrum the sample is illuminated with 4 W of Ar-ion laser (all lines) light. Typically, after approximately 1–1$\frac{1}{2}$ h the light is blocked and the sample is maintained at 77 K. Next, the sample is exposed to CW IR light from a Ninja-4 Clark MXR tunable Ti-Sapphire laser. The IR beam is split with ~1% directed into a 0.25 m scanning monochrometer with resolution ~1 nm. After each exposure to the IR light, the sample is then illuminated with visible light for several minutes until the resistance value prior to IR exposure is recovered. For the electrical measurements, a 1 V or 0.1 V ac signal is applied and phase sensitive detection techniques are used. All data acquisition is automated through the use of a GPIB interface. For the visible photon dose-dependent quenching measurements a 70 mW 1330 nm (YULF) laser is used.

III. RESULTS

Figure 1(a) shows the ρ vs T curve for sample *A* before and after illumination with Ar (all lines) laser light. Significant hysteretic behavior is observed which is typical of PPC/PISC in YBCO. Figure 1(b) shows the response to visible light. When the oxygen content is 6.6, averaged over the first 1000 s during illumination, the ΔR/photon is $1.82 \times 10^{-22}\,\Omega$. When the oxygen content was reduced to 6.26 the ΔR/photon increased to $7.33 \times 10^{-19}\,\Omega$. We are trying to avoid the pitfalls encountered by others[3,4,5,6,8] in characterizing the magnitude of the PPC effect. By expressing our results in terms of ΔR/photon we are making a more general statement about the sample's dc response to visible light than absolute ($\Delta\sigma$) or relative ($\Delta\sigma/\sigma$) changes in conductivity can. We can say unambiguously that the sample's response to visible light was dramatically enhanced by the final annealing process. Before annealing, the net change in the sample's measured resistance due to illumination was ~2–3 Ω at saturation. After the final annealing stage the change in resistance due to illumination is ~14 kΩ. Additionally, the relative change in resistivity ($\Delta\rho/\rho$) increased from 1.6% to 90%.

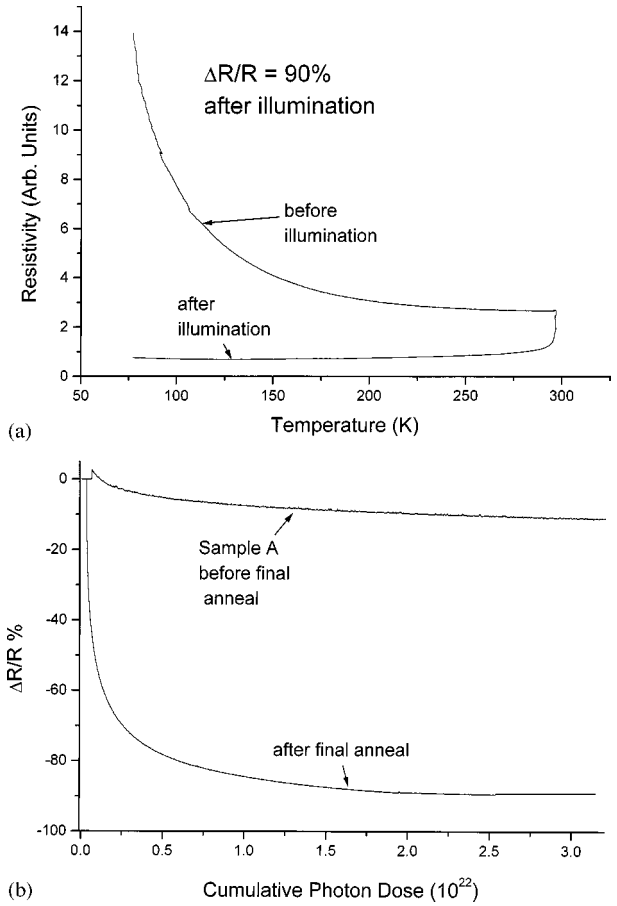

FIG. 1. (a) Resistivity vs temperature curve for sample *A* before and after exposure to ~10^{23} photons of Ar^+ all lines laser. (b) Comparison of sample *A*'s response to visible light before and after annealing. $\Delta R/R$ increases from 1.6 to 90 % and ΔR increases from ~3 Ω to 14 kΩ.

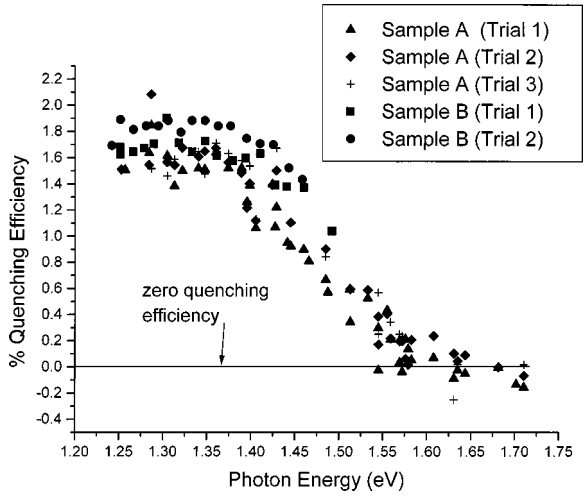

FIG. 2. Quenching efficiency as a function of photon energy for samples *A* and *B*. The meaning of the separate trials is explained in the text.

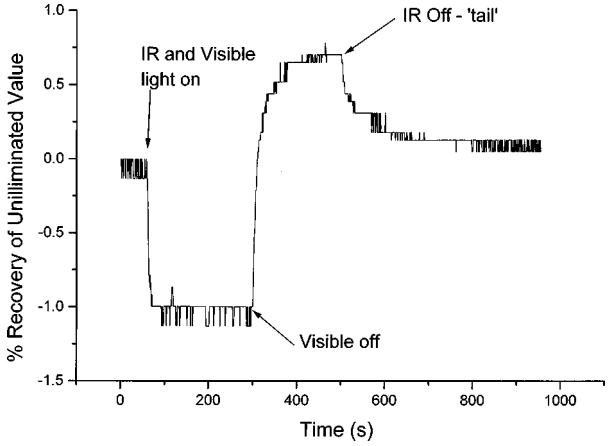

FIG. 3. Simultaneous exposure of sample *B* to visible and IR (1330 nm) light when the PPC effect is near saturation. The character of the response is not appreciably different after exposure to 10^{23} photons as compared with 10^{18}.

Figure 2 shows the quenching spectrum for samples *A* and *B*. For sample *A*, the quenching efficiency was measured between 830 and 990 nm. For sample *B*, the quenching efficiency was measured between 725 and 990 nm. The measurement protocol was slightly different for each sample. Measurements on sample *A* followed the pattern that consecutive trials at a particular wavelength would be performed. In between the sample was exposed to visible illumination in order to fully recover the PPC state. For sample *B* the wavelength of IR light would be incremented in units of 10 nm and the entire spectrum between 830 and 990 nm would be recorded in each run. After each exposure to IR light the sample would be exposed to visible light in order to fully initiate the PPC state again.

The ordinate, quenching efficiency, is defined as the ratio of the change in resistivity due to illumination with IR light to that of the change in resistivity due to illumination with visible light. A 100% quenching efficiency indicates that the value of resistivity prior to illumination with visible light is recovered. For a single wavelength, the largest quenching efficiency observed is ~2%. Broadbanded (1.5–5 μm) IR light has been used in order to achieve a quenching efficiency of 5–10%.[22] This seems to suggest that there is a broad distribution of defects with narrowly spaced energy levels.

Another interesting phenomenon is the ''tail'' that occurs when the IR light is blocked. Figure 3 shows the response of sample *B* to visible (Ar+ all lines, 100 mW) and IR (1330 nm, 70 mW) light. The sample was exposed to IR and visible light simultaneously after having been exposed to 10^{23} visible photons. When the resistivity had not changed for a long time the visible light was blocked. After the response to the IR light is saturated, the IR light is blocked. The resistivity continues to change for some time after the IR light is blocked. As has been described previously,[22] this effect can be attributed to small thermal changes when the light is blocked. Unlike the change in resistivity while the light is on, this change is consistent with the slope of the samples' resistivity vs temperature curve. This ''tail'' also seems to be wavelength independent. However, sample *A* shows different behavior. For wavelengths below 890 nm, an increase in resistance occurs after the light is blocked. Above 890 nm, a decrease occurs. Because of possible ambiguity, the quenching efficiency is defined in such a way as to include the net effect of illumination with IR light. That is, the photoinduced change is taken to be the value of resistance after the sample ''relaxes'' minus the value of resistance before illumination.

Another interesting effect is the response of sample *B* before and after exposure to visible light. As shown in Fig. 4, the resistivity *decreases* during exposure to 887 nm light *before* exposure to visible light. We found this effect to be quite surprising given the results we had encountered previously[22] along with the results of others.[3,8] In the PISC efficiency measurements[3] reported by Kudinov *et al.* the response at 1.4 eV was negligible compared with that at 2.4 eV. Our results contradict this. *After* exposure to visible light in order to induce PPC, illuminating the sample with 887 nm light causes an *increase* in resistance. We undertook a study of the magnitude of quenching as a function of visible photon dose for samples *A* and *C* with the IR wavelength being 1330 nm (0.93 eV). This is shown in Fig. 5 for sample *A*. We also obtained a similar curve for sample *C*. The behavior of the samples is quite surprising in that the character of the

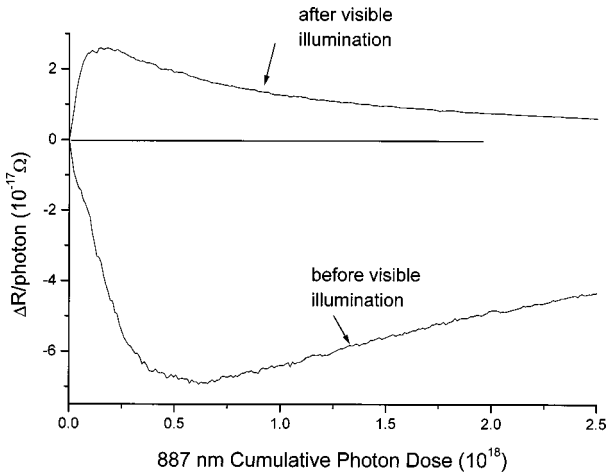

FIG. 4. Response of sample *A* to 887 nm light before and after illumination with visible light.

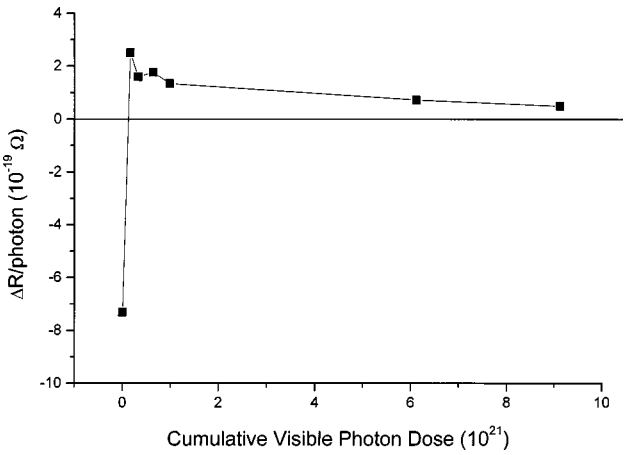

FIG. 5. ΔR per IR photon for sample *A* as a function of visible photon dose. The ordinate changes quickly from large and negative to positive values. A similar curve was obtained for sample *C*.

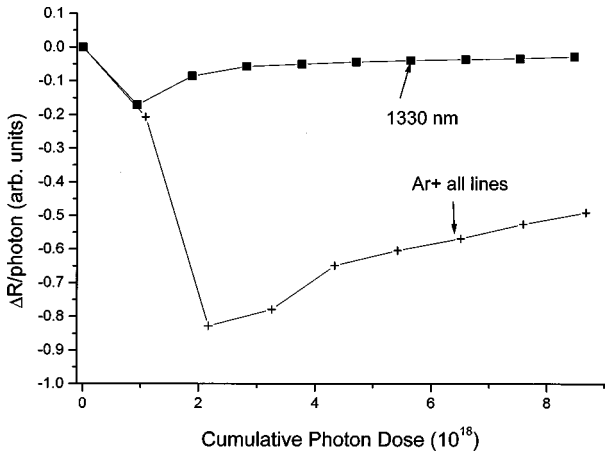

FIG. 6. Comparison of ΔR per photon for 150 mW Ar^+ all lines laser and 70 mW 1330 nm laser. (Sample *C*). Note that the PPC response saturates more quickly for 1330 nm than for visible wavelengths.

response to IR changes dramatically for photon doses as low as $\sim 10^{18}$. Similar effects were observed in samples *D* and *E*.

Figure 3 shows the response of sample *B* when it is nearly saturated in the PPC state. The response to IR light is not appreciably different when it has been exposed to $>10^{23}$ photons as opposed to 10^{18} photons. *This change suggests that defects populate quickly compared with the other dynamics of the PPC effect.* Contributing to this interpretation is the photomodulation spectroscopy[28,29] work done by Taliani and co-workers.[28,29] Photomodulation spectroscopy allows for much more sensitivity than mid-IR reflectivity measurements such as those reported by Widder *et al.*,[20] allowing for resolution to 1 part in 10^4. During low intensity visible illumination Taliani *et al.* recorded the IR spectrum in transmission. Specifically, they recorded fractional changes in transmission between 0.09 and 2.5 eV. They observed two distinct energy bands, one broad ($\sim$1 eV) and centered at 0.8 eV called the high-energy (HE) band. They observed another band having width 0.1 eV at 0.1 eV called the low-energy (LE) band. They found that the LE band grew quickly compared to the HE band when the modulation frequency of the pump beam was decreased, thus suggesting phenomena on two different time scales. Additionally the absorption bleaches above 1.6 eV and saturates around 1.3 eV. We observe the onset of IR quenching at 1.6 eV and saturation around 1.3 eV.

IV. DISCUSSION

Our results seem to suggest that if we extended the wavelength dependence measurements of IR quenching to longer wavelengths we would continue to reproduce the results of Taliani *et al.* Not only do the curves we measured have similar shapes ($-10^4 \Delta T/T$ vs energy and IR quenching efficiency vs energy), but the measurements suggest the coexistence of two phenomena with different time scales. Our results become distinct from those of Taliani *et al.* when we interpret the slower component (LE band) to be related to the motion of the oxygen atoms and the faster component (HE band) to be a true defect band. In addition, the response to IR light before and after visible illumination suggests that the population of defects plays a central role in the character of the PPC response. As shown in Fig. 6, the PPC response to IR wavelengths saturates at a lower photon dose than at visible wavelengths. We suggest that this occurs because there are a smaller percentage of the total defects being populated, i.e., only those with energy equal to and less than 0.93 eV are populated when illuminating with 0.93 eV light. When illuminating with photon energy above 1.6 eV, the total available defects are populated and the response to IR light changes. As shown in the work of Taliani *et al.*, there is photoinduced infrared absorption (PIA) when illuminating with photon energies above 1.6 eV. The similarities between PIA and IR quenching suggest that they are two manifestations of the same phenomenon.

Theoretical treatments of defects on $YBa_2Cu_3O_{6+x}$ have shown that stable *F* centers can form in the CuO_x chains.[30] Earlier work[31] was done concerning the formation of polarons in insulating $YBa_2Cu_3O_{6+x}$. A resonance interaction with $\omega_0 = 200\,\mathrm{cm}^{-1}$ (ω_0 = averaged phonon frequency) was predicted in good agreement with recently observed photoinduced Raman lines[32] in $YBa_2Cu_3O_{6+x}$, which have been identified as CuO_x modes.[33] The relationship between resonant Raman scattering and PPC is unclear. Although at least one author[33] reports stretched-exponential decay of resonant lines during illumination, the bleaching is present in fully oxygenated YBCO which does not exhibit PPC. Additionally, the resonance is very weak for heavily oxygen-deficient material[33] which strongly exhibit PPC. An extensive body of work[34] was done on insulating $YBa_2Cu_3O_{6+x}$ in which the suppression of local tetragonal symmetry by mode bleaching[29,34,35] and the subsequent emergence of local orthorhombic symmetry was seen. Normally, this is taken as evidence of oxygen ordering in the sense that photodoping is seen to mimic increasing the oxygen content. However, it has been shown that changes in the *c* axis and local orthorhombic symmetry can be directly attributed to electron trapping in the chain layers or the conversion of an O^{2-} ion into O^-.[36]

A. Role of defects in PPC

In the light of these results, it seems that there are two roles that defects may play in PPC in YBCO. First, they may

be an independent phenomenon associated with chain oxygen vacancies in YBCO. Their existence has been investigated and shown to be plausible.[5,21,30,36] As a distinct mechanism of PPC, their contribution may be at most 10% compared to oxygen ordering.[22] This estimate is inferred from the fact that IR quenching can only cause a small change in resistivity when compared with that caused by visible light. However, it seems unlikely to us that the mechanism responsible for IR quenching and PPC are unrelated. First, they have overlapping spectral features. That alone is not convincing, but the fact that the overlapping spectral features depend on one another is suggestive. IR wavelengths initiate PPC before exposure to visible light and partially quench it after, suggesting to us that the mechanisms for both phenomena are intimately related.

A more comprehensive description of PPC could include defects as precursors to oxygen ordering during illumination with visible light. The trapped charges modify the local electric-field distribution which leads to induced dipole moments. These dipoles create the necessary impetus for the movement of oxygen.[17] In this model PPC would result from the combined action of two mechanisms. First, the population of defects would occur quickly resulting in changes in local structure. Secondly, as a result of the modification of local fields, structural changes would occur over a much longer time scale that reflect the periodicity of the lattice. Then, PPC is understood as the sum effect of an electronic contribution (defects, fast) and a lattice contribution (ordering, slow). This model can account for the quicker saturation of IR quenching as well as the much smaller change in resistance when compared to PPC. Further, this view on the role of defects is consistent with almost any model that contains oxygen ordering and actually enhances them by providing a clue as to the precursor of this ordering.

B. Timescales in PPC

After illumination with visible light, and during illumination with IR light the change in resistance as a function of time can be fit with a stretched exponential.[22] Obviously, the saturation parameters are different for IR quenching and PPC. The dispersion parameters are expected to vary as well although no formal temperature-dependent measurements have been carried out. Difficulty arises in assigning a physical meaning to the parameters involved in these fits. In fact, the validity of their physical meaning at all has been called into question. For example, semiconducting[3] samples *only* were observed to have a thermal barrier of width $\sim$1 eV in one study, whereas in another study[23] this barrier existed for metallic samples as well. Additionally, the trap size and width evolve oppositely with temperature in both of these studies. We can only speculate as to the reasons for this discrepancy. IR quenching is considerably weaker in metallic samples than in semiconducting ones, and is nearly impossible to observe for O contents greater than 6.6. We attribute this to a decreasing number of traps whose excitation gives a negligible contribution to the macroscopic resistivity. However, this does not shed light on the aforementioned discrepancy regarding the Kohlrausch parameters involved in the stretched-exponential fit. The stretched-exponential fit implies a distribution of lifetimes in the system. We believe the shorter time constants are involved with the population of defects (as implied by IR quenching), and the longer time constants are those due to structural changes. Even though the physical meaning of the parameters involved in the fit is somewhat blurred, the overall picture remains consistent: a fast change that is primarily electronic accompanied by slower changes that are structural.

V. CONCLUSION

When oxygen-deficient YBCO is illuminated with IR radiation, the response to IR wavelengths is dramatically different depending on whether or not the sample has been exposed to visible light. Before the sample is exposed to visible light, IR light initiates the PPC state. After the sample is exposed to visible light, IR light partly quenches the PPC state. Oxygen ordering alone cannot account for the existence of IR quenching nor the fact that it saturates for one part in 10^5 of the photon dose required for saturation of the PPC effect. The IR quenching efficiency is not substantially different after illumination with 10^{18} photons as opposed to 10^{23}. Were this simply a manifestation of the PPC effect, one would expect the IR quenching efficiency to be proportional in some way with the visible photon dose. One sees this with the changes in the c axis[10,11] ($\Delta c/c$) as measured by XRD during illumination, i.e., it follows stretched-exponential decay just as the resistivity. However, the magnitude of IR quenching does not appear to be related to the cumulative visible photon dose unless the functional form is on a scale vastly smaller than the PPC effect. In that case, this result would still be suggestive of two phenomena on different time scales. Different time dynamics exhibited by IR quenching and PPC in YBCO, coupled with the observed wavelength dependence of IR quenching, suggest that defects may play an important role in PPC.

ACKNOWLEDGMENTS

This work was supported by The National Science Foundation under Grants Nos. ECS-96223-13 and EEC-95274911. Helpful discussions with J. M. Joseph and T. A. Tyson are acknowledged. We thank A. Heilman for assistance with Ag contacts. We are grateful to H. Grebel for use of the 1.3 μm laser.

*Electronic address: dmb8027@megahertz.njit.edu, bubbdanny@home.com

[1] A. I. Kirulyik, N. M. Kreines, and V. I. Kudinov, Pisma Zh. Eksp. Teor. Fiz. **52**, 696 (1990) [JETP Lett. **52**, 49 (1990)].

[2] V. I. Kudinov, N. M. Kreines, A. I. Kirulyik, R. Laiho, and E. Lähderanta, Phys. Lett. A **151**, 358 (1990).

[3] V. I. Kudinov, I. L. Chaplygin, N. M. Kreines, A. I. Kirulyik, R. Laiho, E. Lähderanta, and C. Ayache, Phys. Rev. B **47**, 9017 (1993).

[4] E. Osquiguil, M. Maenhoudt, B. Wuyts, Y. Bryunseraede, D. Lederman, and I. K. Schuller, Phys. Rev. B **49**, 3675 (1994).

[5] J. Hasen, D. Lederman, I. K. Schuller, V. Kudinov, M. Maen-

houdt, and Y. Bryunseraede, Phys. Rev. B **51**, 1342 (1995).
[6] J. Hasen, Ph.d. Thesis, University of California San Diego, 1995.
[7] G. V. Uimin, V. F. Gentmakher, A. M. Neminsky, L. A. Novomlinsky, D. V. Shovkum, and P. Brüll, Physica C **192**, 481 (1992).
[8] K. Tanabe, S. Kubo, F. Hosseini Teherani, H. Asano, and M. Suzuki, Phys. Rev. Lett. **72**, 1537 (1994).
[9] K. Kawamoto and I. Hirabayashi, Phys. Rev. B **49**, 3655 (1995).
[10] T. A. Tyson, J. F. Federici, D. Chew, A. R. Bishop, L. Furenlid, W. Savin, and W. Wilber, Physica C **292**, 163 (1997).
[11] D. Lederman, J. Hasen, I. K. Schuller, E. Osquiguil, and Y. Bruynseraede, Appl. Phys. Lett. **64**, 652 (1994).
[12] J. D. Jorgenson, M. A. Beno, D. G. Hinks, L. Soderholm, K. J. Volin, C. U. Segre, K. Zhang, and M. S. Kleefisch, Phys. Rev. B **36**, 3608 (1987).
[13] D. J. Werder, C. H. Chen, R. J. Cava, and B. Battlogg, Phys. Rev. B **38**, 5130 (1988).
[14] D. J. Werder, C. H. Chen, R. J. Cava, and B. Battlogg, Phys. Rev. B **37**, 2317 (1987).
[15] B. W. Veal, A. P. Paulikas, Hoydoo You, Hao Shi, Y. Fang, and J. W. Downey, Phys. Rev. B **42**, 6305 (1990).
[16] J. Kirchner, M. Cardona, A. Zibold, K. Widder, and H. P. Geserich, Phys. Rev. B **48**, 9864 (1993).
[17] G. Grigelionis, E. E. Tornau, and A. Rosengren, Phys. Rev. B **53**, 425 (1996).
[18] E. Osquiguil, M. Maenhoudt, B. Wuyts, Y. Bruynseraede, D. Lederman, and I. K. Schuller, Phys. Rev. B **49**, 3675 (1994).
[19] S. Lapinskas, A. Rosengren, and E. Tornau, Physica C **199**, 91 (1991).
[20] K. Widder, J. Münzel, M. Göppert, D. Lüerssen, R. Becker, A. Dinger, H. P. Geserich, C. Klingshern, M. Kläser, G. Müller-Vogt, J. Geerk, and V. M. Berkalov, Physica C **300**, 115 (1997).
[21] J. F. Federici, D. Chew, B. Welker, W. Savin, J. Gutierrez-Solana, T. Fink, and W. Wilber, Phys. Rev. B **52**, 15 592 (1995); also, Refs. 15–25.
[22] D. C. Chew, J. F. Federici, J. Gutierrez-Solona, G. Molina, W. Savin, and W. Wilber, Appl. Phys. Lett. **69**, 3260 (1996).
[23] W. Markowitsch, C. Stockinger, W. Göb, W. Lang, W. Kula, and R. Sobolewski, Physica C **265**, 187 (1996).
[24] Proceedings of the International Conference on HTSC, Interlaken 1988, edited by J. Müller and J. L. Olsen [Physica C **153-5** (1988)].
[25] Jinhua He and Keikchi Nakamura, Phys. Rev. B **48**, 7554 (1993).
[26] J. Zhang, R. A. Gardiner, P. S. Kirlin, R. W. Boerstler, and J. Steinbeck, Appl. Phys. Lett. **61**, 2884 (1992).
[27] S. Degoy, J. Jiménez, P. Martin, O. Martinez, A. C. Prieto, D. Chambonnet, C. Audry, C. Belouet, and J. Perrière, Physica C **256**, 291 (1997).
[28] X. Wei, L. Chen, Z. V. Vardeny, C. Taliani, R. Zamboni, A. J. Pal, and G. Ruani, Physica C **162-4**, 1109 (1989).
[29] C. Taliani, A. J. Pal, G. Ruani, R. Zamboni, X. Wei, and Z. V. Vardeny, *Electronic Properties of High T_c Superconductors and Related Compounds*, edited by H. Kuzmany, M. Mehring, and J. Fink (Springer-Verlag, Berlin, 1990).
[30] N. Kristoffel and P. Rubin, J. Phys.: Condens. Matter **10**, L127 (1998).
[31] D. Mihailović, C. M. Foster, K. Voss, and A. J. Heeger, Phys. Rev. B **42**, 7989 (1990).
[32] A. G. Panfilov, A. I. Rykov, and S. Tajima, Phys. Rev. B **58**, 12 459 (1998).
[33] M. Käll, M. Osada, M. Kakihana, L. Börjesson, T. Frello, J. Madsen, N. H. Andersen, R. Liang, P. Dosanjh, and W. N. Hardy, Phys. Rev. B **57**, 14 072 (1998).
[34] Y. H. Kim, C. M. Foster, A. J. Heeger, S. Cox, and G. Stucky, Phys. Rev. B **38**, 6478 (1988).
[35] D. Mihailović, C. M. Foster, K. Voss, T. Mertelj, I. Poberaj, and N. Herron, Phys. Rev. B **44**, 237 (1991).
[36] N. Kristoffel and P. Rubin, Phys. Rev. B **54**, 9074 (1996).